Available online at www.sciencedirect.com
ScienceDirect
International Communications in Heat and Mass Transfer 33 (2006) 1063 – 1070
International Communications in HEAT and MASS TRANSFER
www.elsevier.com/locate/ichmt

Mathematical determination of emissivity and surface temperature of aluminum alloys using multispectral radiation thermometry ☆

Chang-Da Wen, Issam Mudawar *

Boiling and Two-phase Flow Laboratory, School of Mechanical Engineering, Purdue University, West Lafayette, IN 47907, USA

Available online 13 July 2006

Abstract

A relatively simple emissivity model has recently been shown to effectively capture the parameteric effects of wavelength, temperature, alloy and surface roughness on the emissivity of aluminum surfaces. In the present study, a mathematical method is developed for determining both the empirical constant in the emissivity model and the surface temperature based on spectral radiance measurements. This study proves the relationship between reflectance ratio and optical roughness is by no means universal, and the complex effects of wavelength, temperature, alloy and surface roughness are more accurately captured with the aid of a multispectral emissivity model.

Keywords: Multispectral radiation thermometry; Emissivity; Temperature measurement

1. Introduction

Producing aluminum alloy parts with superior microstructure and mechanical properties requires a thorough understanding of both metallurgical transformation kinetics and temperature-time heating/cooling rate. The temperature-time characteristics are process specific, dictated by part mass, shape, and transit speed. The final microstructure and hence mechanical properties of the aluminum part are dictated by the interrelation between the temperature-time characteristics and the transformation kinetics of the alloy. This interrelation therefore has a strong bearing on the part's quality, reproducibility, and cost.

With such a strong dependence of aluminum processes on temperature, accurate determination of the part's temperature is paramount. While surface contact sensors are presently used throughout the aluminum industry, the fast transit of parts in processes such as extrusion and rolling renders these sensors both inaccurate and potentially damaging to the part's surface. Non-contact radiation thermometry is highly desirable in those situations, provided such instrumentation can achieve the desired measurement accuracy. Given the low emissivity values of most aluminum surfaces, the signal detected by a radiation thermometer is typically very weak, which explains the challenge in obtaining accurate temperatures for aluminum.

☆ Communicated by W.J. Minkowycz.

* Corresponding author.
E-mail address: mudawar@ecn.purdue.edu (I. Mudawar).

0735-1933/$ - see front matter © 2006 Elsevier Ltd. All rights reserved.
doi:10.1016/j.icheatmasstransfer.2006.05.010

Nomenclature

α_0	Empirical coefficient in MRT model
c_1	First thermal radiation constant
c_2	Second thermal radiation constant
$L_{\lambda,b}$	Spectral intensity of blackbody radiation
$L_{\lambda,\mathrm{gen}}$	Generated spectral radiation intensity
$L_{\lambda,\mathrm{meas}}$	Measured spectral radiation intensity
n	Number of unknown coefficients in emissivity model
N	Minimum number of wavelengths required in MRT model
T	Surface temperature

Greek Symbols

ε_n	Normal spectral emissivity
ε_r	Emissivity of rough surface
ε_s	Emissivity of smooth surface
ε_λ	Spectral emissivity
λ	Wavelength
ρ_r	Reflectance of rough surface
ρ_p	Reflectance of polished surface
σ	Root-mean-square (rms) surface roughness
χ^2	Least-squares error

Subscripts

b	Blackbody
gen	Generated
meas	Measured
n	Normal
r	Rough
p	Polished
λ	Spectral

Inferring surface temperature can be accomplished by three categories of radiation thermometry which utilize radiance measurements at different numbers of wavelength: spectral, dual-wavelength and multispectral. Spectral radiation thermometry requires radiance measurement at one wavelength and a constant emissivity value to infer the surface temperature. Dual-wavelength radiation thermometry (DWRT) employs radiance measurements at two wavelengths and an emissivity compensation algorithm. Multispectral radiation thermometry (MRT) employs radiance measurements at three or more wavelengths and an emissivity model. The latter method is favored for aluminum temperature measurements because of its effectiveness at capturing the complex emissivity behavior of practical aluminum surfaces [1]. The present study is based on the MRT method.

Recently, the authors of the present study examined the emissivity characteristics of polished and roughened aluminum alloy surfaces relative to wavelength, temperature, heating time, and alloy [2,3]. Eighteen MRT emissivity models were tested for accuracy at inferring surface temperature. A relatively simple mathematical model, the exponential of a linear first order function of $\sqrt{\lambda}$, provided the best overall compensation.

The present study examines the complex parametric trends of emissivity of aluminum surfaces with wavelength, temperature, alloy and surface roughness, and provides a mathematical method for determining both the empirical constant in the MRT emissivity model and the surface temperature based on spectral radiance measurements.

2. Experimental methods

A Fast Infrared Array Spectrometer (FIAS) Model ES100 made by Spectraline Inc. was optically aligned in front of the test sample with the aid of a He–Ne laser. This instrument has the capability to simultaneously measure 160 discrete spectral radiation intensity values over the range of 1.8 to 4.9 μm.

As shown in Fig. 1(a), the sample heating assembly consisted of a large aluminum block fitted with four cartridge heaters and encased in a ceramic fiber insulating blanket. The heating assembly rested on a two-dimensional translation stage. The aluminum test sample was held in contact with the aluminum heating block by an insulating flange as shown in Fig. 1(b). The test surface area of the sample was 15×15 mm^2. A thermocouple was inserted 1 mm behind the test surface to measure the sample's temperature. The temperature gradient between the thermocouple bead and the surface was negligible because of the high conductivity of the aluminum samples. The thermocouple output was recorded simultaneously with that of the spectrometer once the sample temperature reached steady state. The thermocouple measurement was calibrated by an Omega CL1000 hot point dryblock calibrator. The thermocouple readout from the digital thermometer was corrected by the calibration offset, which was less than 1.6 K for a surface temperature of 523 K.

Four test samples, AL 1100, AL 2024, AL 7075, AL 7150, covered broad ranges of aluminum alloys and applications. Two different types of surface conditions were examined: polished and roughened with 14 μm grit paper. The flat mirror-like polished surface was created by a series of five polishing wheels with increasing finer grit and particle size (320 grit SiC, 400 grit SiC, 600 grit SiC, diamond compound, Gamma alumina).

3. Application of MRT emissivity models

Two different mathematical techniques of MRT are generally used to infer surface temperature. The first is the exact technique which employs an emissivity model with n unknown coefficients and radiation intensity

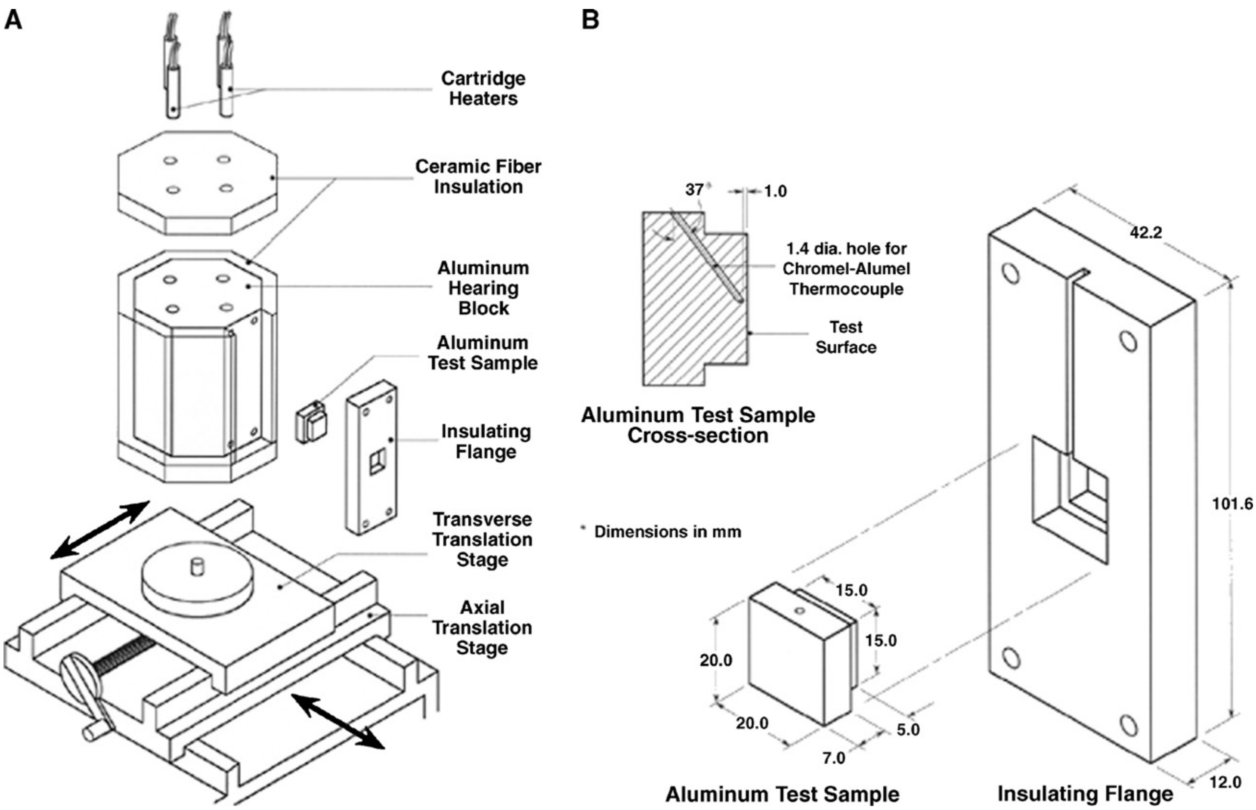

Fig. 1. Construction of (a) sample heating assembly and (b) test sample and insulating flange.

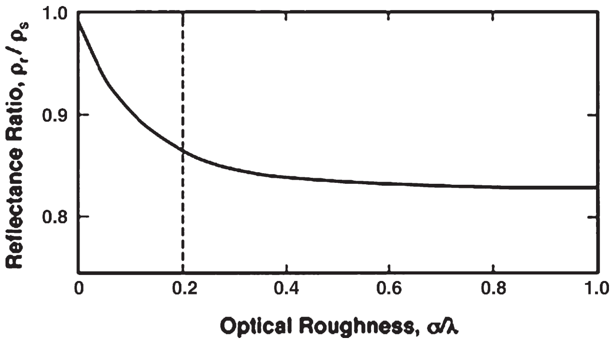

Fig. 2. Ratio of normal hemispherical reflectance versus optical roughness for aluminum coated ground glass (adapted from [8]).

measurements at $n+1$ wavelengths. Coates [4] and Doloresco [5] concluded the exact technique might cause over-fitting and result in large errors when using more than three wavelengths. The other method, which can overcome the over-fitting problem, is the least-squares technique. It employs least squares fitting of the measured intensities to simultaneously deduce both the temperature and the values of the empirical coefficients in the emissivity model. The least-squares technique requires spectral intensity measurements at a minimum of $N=n+2$ wavelengths when employing an emissivity model with n unknown coefficients. A modified linear least-squares technique is used to simplify calculations where the emissivity model has an exponential form.

As indicated earlier, the authors proved the following exponential emissivity function provides the best overall compensation for different allow samples, wavelengths, temperatures, and surface roughnesses [2,3],

$$\varepsilon_\lambda = \exp(a_0\sqrt{\lambda}). \tag{1}$$

In the linear least-squares technique, the temperature and unknown emissivity coefficient are determined by minimizing the chi-squared (χ^2) value given by

$$\chi^2 = \sum_{i=0}^{n} (\ln L_{\lambda,\mathrm{meas},i} - \ln L_{\lambda,\mathrm{gen},i})^2, \tag{2}$$

where $L_{\lambda,\mathrm{meas},i}$ is the measured spectral intensity and $L_{\lambda,\mathrm{gen},i}$the intensity value generated according to the Planck distribution.

$$L_{\lambda,\mathrm{gen},}(\lambda,T) \cong \varepsilon_\lambda(\lambda) L_{\lambda,b}(\lambda,T) = \varepsilon_{\lambda(\lambda)} \frac{c_1}{\lambda^5(e^{c_2/\lambda T}-1)}. \tag{3}$$

The Planck distribution in the above equation can be approximated by Wien's formula.

$$L_{\lambda,b}(\lambda,T) \frac{c_1}{\lambda^5(e^{c_2/\lambda T}-1)} \cong \frac{c_1}{\lambda^5(e^{c_2/\lambda T})}. \tag{4}$$

This approximation is used to yield a set of equations that are linear with respect to temperature and the unknown emissivity coefficient.

$$\begin{aligned}\chi^2 &= \sum_{i=0}^{n} \left\{ \ln L_{\lambda,\mathrm{meas},i} - \ln\left[\exp(a_0\sqrt{\lambda_i}) \frac{c_1}{\lambda_i^5(e^{c_2/\lambda_i T})}\right]\right\}^2 = \sum_{i=0}^{n}\left(\ln L_{\lambda,\mathrm{meas},i} - a_0\sqrt{\lambda_i} - \ln\frac{c_1}{\lambda_i^5} + \frac{c_2}{\lambda_i T}\right)^2 \\ &= \sum_{i=0}^{n}\left(\ln\frac{L_{\lambda,\mathrm{meas},i}\lambda_i^5}{c_1} - a_0\sqrt{\lambda_i} + \frac{c_2}{\lambda_i}T^{-1}\right)^2. \end{aligned} \tag{5}$$

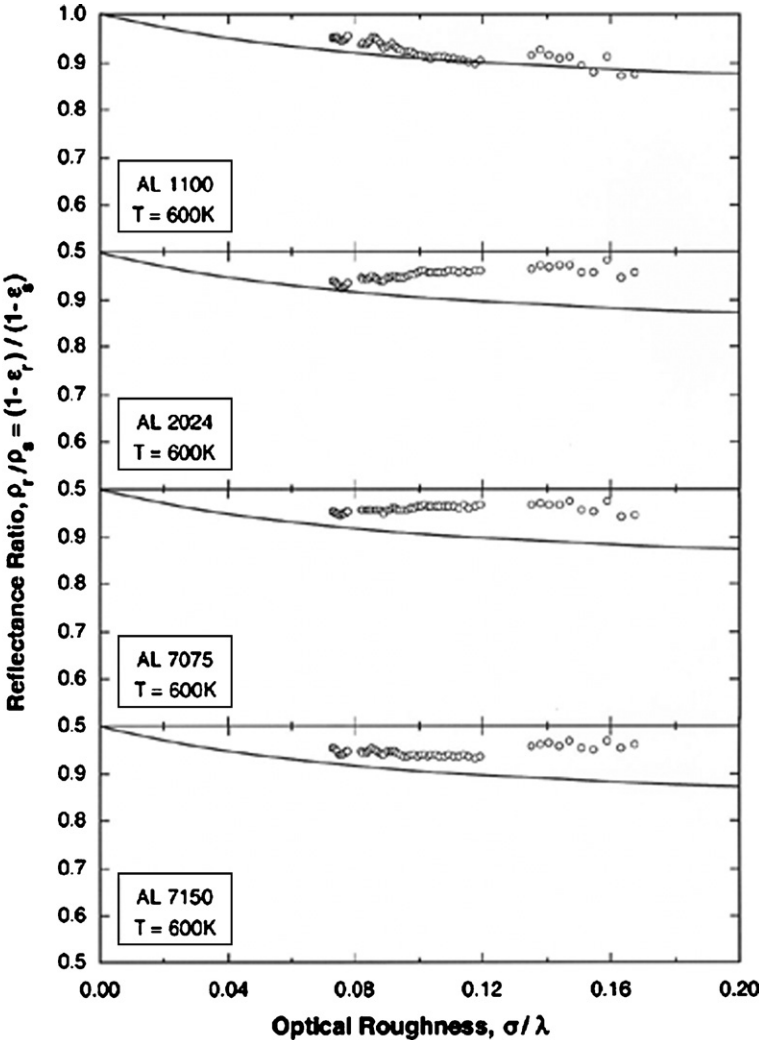

Fig. 3. Present normal hemispherical reflectance values versus optical roughness for different alloys at 600 K compared with Eq. (9).

Chi-squared is minimized by setting $\dfrac{\partial \chi^2}{\partial a_0} = \dfrac{\partial \chi^2}{\partial T^{-1}} = 0$,

$$\frac{\partial \chi^2}{\partial a_0} = 0 = \sum_{i=1}^{N} 2\left(\ln\frac{L_{\lambda,\mathrm{meas},i}\lambda_i^5}{c_1} - a_0\sqrt{\lambda_i} + \frac{c_2}{\lambda_i}T^{-1}\right)(-\sqrt{\lambda_i}) \tag{6}$$

and

$$\frac{\partial \chi^2}{\partial T^{-1}} = 0 = \sum_{i=1}^{N} 2\left(\ln\frac{L_{\lambda,\mathrm{meas},i}\lambda_i^5}{c_1} - a_0\sqrt{\lambda_i} + \frac{c_2}{\lambda_i}T^{-1}\right)\left(\frac{c_2}{\lambda_i}\right). \tag{7}$$

From Eqs. (6) and (7), the unknown coefficient a_0 and T can be determined by solving the following system of linear algebraic equations,

$$\begin{bmatrix} \lambda_i & -\dfrac{c_2}{\sqrt{\lambda_i}} \\ \dfrac{c_2}{\sqrt{\lambda_i}} & -\left(\dfrac{c_2}{\lambda_i}\right)^2 \end{bmatrix} \cdot \begin{bmatrix} a_0 \\ T^{-1} \end{bmatrix} = \begin{bmatrix} \sqrt{\lambda_1}\ln\dfrac{L_{\lambda,\mathrm{meas},i}\lambda_i^5}{c_1} \\ \dfrac{c_2}{\lambda_i}\ln\dfrac{L_{\lambda,\mathrm{meas},i}\lambda_i^5}{c_1} \end{bmatrix}. \tag{8}$$

4. Results and discussion

Theoretical emissivity principles are generally categorized by optical roughness, σ/λ, the ratio of root-mean-square (rms) surface roughness to wavelength. Two broad categories of surfaces can be identified: optically smooth (ideal) and rough (real). Rough surfaces can be further broken down into a *specular region*, corresponding to $0<\sigma/\lambda<0.2$, an *intermediate region*, $0.2<\sigma/\lambda<1$, and a *geometrical region*, $\sigma/\lambda>1$.

The roughness of the present aluminum samples falls in the specular region. In most theoretical studies of this region, the reflection of incident radiation is assumed to be specular, i.e., the angle of reflection is equal to the angle of incidence, and the diffraction theory is used to predict the effects of surface roughness on emissivity [6–8]. For a Gaussian distribution of surface heights, the relationship between reflected radiation and optical roughness has been shown both theoretically [9,10] and experimentally [11,12] to follow an exponential decay function of σ/λ.

$$\rho_r = \rho_s \exp\left[-\left(\frac{4\pi\sigma}{\lambda}\right)^2\right], \tag{9}$$

where ρ_r is the normal-hemispherical reflectance for a rough surface and ρ_s for a polished surface. Fig. 2 shows a curve fit of experimental results for the reflectance ratio for a real surface to that for a smooth surface versus optical roughness for aluminum-coated ground glass [13]. Shown is a decrease in reflectance with increasing surface roughness. Since $\rho_r = 1-\varepsilon_n$, where ε_n is the

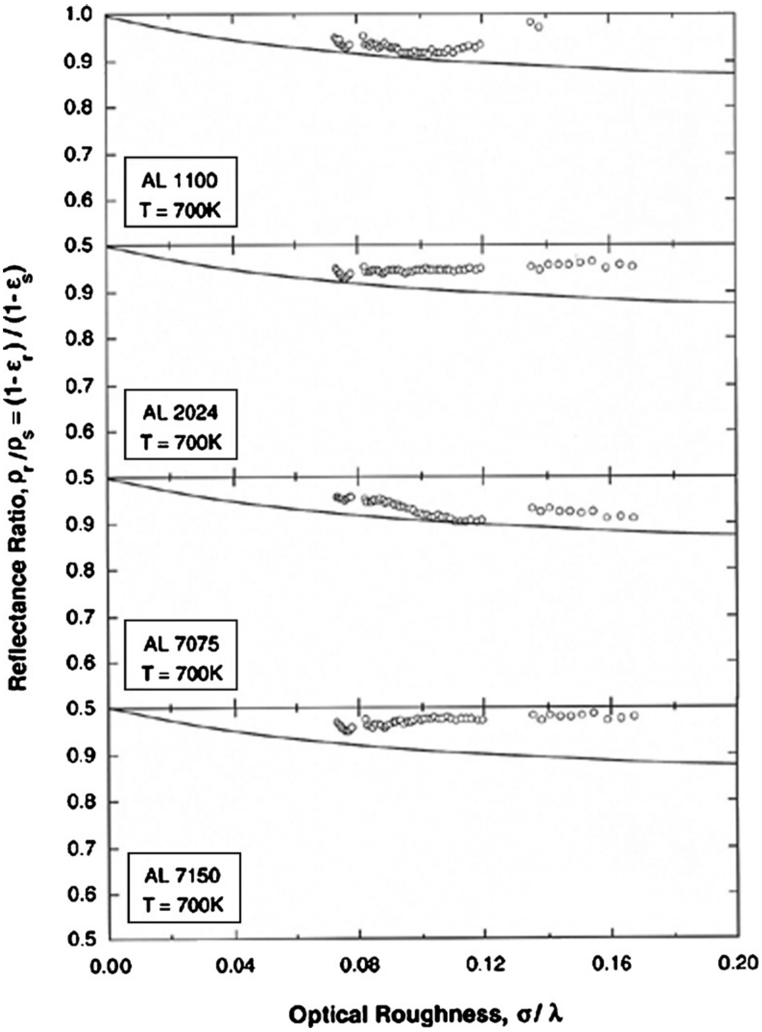

Fig. 4. Present normal hemispherical reflectance values versus optical roughness for different alloys at 700 K compared with Eq. (9).

Table 1
Absolute error in inferred temperature of aluminum alloy samples using MRT emissivity model

T	N [a]	Wavelength (micrometers)											
		2.05–3.43				3.50–4.72				2.05–4.72			
		AL 1100	AL 2024	AL 7075	AL 7150	AL 1100	AL 2024	AL 7075	AL 7150	AL 1100	AL 2024	AL 7075	AL 7150
Polished													
600 K	N		43.2	48.7	36.2					−5.2	0.5	4.6	−7.8
	$N+1$		46.1		39.3					−9.4	−1.5	2.7	−10.2
	$N+2$				44.2					−9.7	−2.1	2.4	−11.1
700 K	N		−15.0	−26.5	−26.7					−6.8			−47.4
	$N+1$		−4.4	−11.0	−20.9					−11.2			−47.4
	$N+2$		−4.0	−12.4	−19.6					−10.6			−46.8
Roughened with 14 mm grit paper													
600 K	N	33.7	31.1	41.9	12.8					3.5	−7.2	1.6	−12.4
	$N+1$	35.2	32.1	43.0	13.0					2.1	−9.7	−0.4	13.5
	$N+2$	36.6	34.5	44.8	16.4					2.1	−10.0	−0.6	−14.1
700 K	N	−34.6	−25.1	−27.5	−29.9					−49.2		−47.5	−49.7
	$N+1$	−31.8	−21.3	−24.1	−26.9					−49.8		−48.6	
	$N+2$	−30.7	−19.7	−22.7	−24.2					−49.3		−48.3	

Missing values correspond to errors beyond ±50 K.

[a] N is the minimum number of the wavelengths required in MRT model, which is equal to number of unknown coefficients in model plus two.

normal emissivity, Fig. 2 shows emissivity increases with increasing roughness. This effect is appreciable in the specular region ($0<\sigma/\lambda<0.2$) and far weaker as σ/λ approaches unity (onset of geometrical region).

Figs. 3 and 4 show measured reflectance plotted against optical roughness for temperatures of 600 and 700 K, respectively. Also so shown in the same figures are predictions based on Eq. (9). The present data fall in the specular region ($0<\sigma/\lambda<0.2$), and show different trends for different alloys and different temperatures. For example, Fig. 3 shows both higher values of reflectance ratio and milder variation with optical roughness for AL 7075 than for AL 1100. These trend variations are even more pronounced at 700 K, Fig. 4. These results prove the relationship between reflectance ratio and optical ratio depicted in Fig. 2 is by no means universal since it does not account for the complex reflectance variations of aluminum alloys with wavelength, temperature, alloy, and surface roughness.

This also proves the effects of these parameters can be more thoroughly examined by using an MRT emissivity model. Table 1 shows absolute errors in the inferred temperatures for the polished surface and the 14 μm roughened surface using the MRT model. Missing values in the table correspond to errors beyond ±50 K and serve to help point out useful trends in the inferred temperature. The table includes results for four aluminum alloys, AL 1100, AL 2024, AL 7075 and AL 7150, two temperatures, 600 and 700 K, and three spectral ranges between 2.05 to 4.72 μm. The least squares technique requires a minimum number of wavelengths, N, equal to the number of unknown coefficients in the emissivity model plus two. Since the MRT model includes only one empirical constant, $N=3$. Table 1 also shows results for the minimum number of wavelength plus one and plus two to explore the effects of number of wavelengths on temperature predictions. Increasing the number of wavelengths above the minimum value does not appear to enhance the accuracy of the temperature predictions. Table 1 also shows results for three spectral ranges: a relatively short range of 2.05–3.43 μm, a long range of 3.50–4.72 μm, and a combined range of 2.05–4.72 μm. Notice how acceptable results are realized in the short and combined ranges but not the intermediate range. This shows broadening the spectral range does not always enhance measurement accuracy.

These results prove the present MRT model is effective at capturing the complex emissivity trends of aluminum surfaces relative to wavelength, temperature, alloy and surface roughness.

5. Conclusions

This study examined the parameteric effects of wavelength, temperature, alloy and surface roughness on the emissivity of aluminum surfaces. Used with the least-squares MRT technique, a relatively simple emissivity model, the exponential of a linear first order function of $\sqrt{\lambda}$, is shown to effectively capture these trends for four aluminum alloys, two surface roughnesses, and two temperatures over an overall spectral range of 2.05 to 4.72 μm. This study also provided a mathematical method for determining both the empirical constant in the emissivity model and the surface temperature based on the spectral radiance measurements. The present findings show the relationship between reflectance ratio with optical roughness for $0<\sigma/\lambda<0.2$ is by no means universal, and the complex effects of wavelength, temperature, alloy and surface roughness are more accurately captured with the aid of the MRT emissivity model.

References

[1] M.A. Pellerin, Multispectral radiation thermometry for industrial applications, Ph.D. Thesis, Purdue University, West Lafayette, IN, 1999.

[2] C. Wen, I. Mudawar, Emissivity characteristics of polished aluminum alloy surfaces and assessment of multispectral radiation thermometry (MRT) emissivity models, International Journal of Heat and Mass Transfer 48 (2005) 1316–1329.

[3] C. Wen, I. Mudawar, Emissivity characteristics of roughened aluminum alloy surfaces and assessment of multispectral radiation thermometry (MRT) emissivity models, International Journal of Heat and Mass Transfer 47 (2005) 3591–3605.

[4] P.B. Coates, Multi-wavelength pyrometry, Metrologia 17 (1981) 103–109.

[5] B.K. Doloresco, Review of multispectral radiation thermometry and development of constrained minimization method, M.S. Thesis, Purdue University, West Lafayette, IN, 1986.

[6] R. Siegel, J.R. Howell, Thermal Radiation Heat Transfer, McGraw–Hill, New York, NY, 1981.

[7] D.P. DeWitt, J.C. Richmond, Thermal radiative properties of materials, in: D.P. DeWitt, G.D. Nutter (Eds.), Theory and Practice of Radiation Thermometry, John Wiley, New York, NY, 1988.

[8] M.J. Haugh, Radiation thermometry in the aluminum industry, in: D.P. DeWitt, G.D. Nutter (Eds.), Theory and Practice of Radiation Thermometry, John Wiley, New York, NY, 1988.

[9] H. Davis, Reflection of electromagnetic waves from rough surfaces, Proceedings of the Institute of Electrical Engineers, vol. 101, 1954, pp. 209–213.

[10] J.O. Porteus, Relation between the height distribution of a rough surface and the reflection of normal incidence, Journal of the Optical Society of America 53 (1963) 1394–1402.

[11] H.E. Bennett, J.O. Porteus, Relation between surface roughness and specular reflectance at normal incidence, Journal of the Optical Society of America 51 (1961) 123–129.

[12] H.E. Bennett, Specular reflectance of aluminized ground glass and the height distribution of surface irregularities, Journal of the Optical Society of America 53 (1963) 1389–1394.

[13] R.C. Birkebak, E.R.G. Eckert, Effect of metal surface on the angular distribution of monochromatic reflected radiation, Transactions of ASME 87C (1965) 85–94.